Selecting the Lorenz Parameters for Wideband Radar Waveform Generation

Matt S. Willsey[+], Kevin M. Cuomo[†], and Alan V. Oppenheim[‡]

Abstract

Radar waveforms based on chaotic systems have occasionally been suggested for a variety of radar applications. In this paper, radar waveforms are constructed with solutions from a particular chaotic system, the Lorenz system, and are called Lorenz waveforms. Waveform properties, which include the peak autocorrelation function side-lobe and the transmit power level, are related to the system parameters of the Lorenz system. Additionally, scaling the system parameters is shown to correspond to an approximate time and amplitude scaling of Lorenz waveforms and also corresponds to scaling the waveform bandwidth. The Lorenz waveforms can be generated with arbitrary time lengths and bandwidths and each waveform can be represented with only a few system parameters. Furthermore, these waveforms can then be systematically improved to yield constant-envelope output waveforms with low autocorrelation function sidelobes and limited spectral leakage.

Index Terms

Radar, Waveforms, Wideband, Chaos, Lorenz, Time-Scaling.

I. INTRODUCTION

Due to the aperiodic nature of chaotic dynamics, chaotic systems can be used to generate signals with low autocorrelation sidelobes. Since many radar systems utilize the matched filter to achieve high range resolution and maximize the SNR in Gaussian noise [North, 1963], low autocorrelation function sidelobes help prevent false alarms and prevent stronger returns from masking the presence of weaker returns. Furthermore, for wide bandwidths, these chaotic waveforms lead to high range resolution [Rihaczek, 1996].

Many waveform design techniques have been proposed using chaotic systems with amplitude or frequency/phase modulation (see, for example, [Venkatasubramanian & Leung, 2005; Lukin, 2001; Flores, et al., 2003]). The contribution of this paper is to develop a specific chaotic system, the Lorenz system [Lorenz, 1963], for waveform

generation by appropriately selecting the system parameters. Specifically, scaling the Lorenz parameters is shown in Section II to approximately scale the Lorenz solutions in time and amplitude, which can therefore be used to set the bandwidth of the Lorenz waveforms. The time-scaling property also allows a decoupling of the three system parameters into one parameter that controls the bandwidth and two parameters that control other waveform properties. The two-dimensional parameter space is explored in Section III to determine how these parameters affect various waveform properties. Whereas techniques with amplitude modulation often sacrifice sensitivity and techniques with frequency/phase modulation often lead to spectral leakage (due to abrupt transitions in instantaneous frequency), the resulting Lorenz waveforms can be improved using the procedure in [Willsey et al., 2010] to yield high-power waveforms with limited spectral leakage. Moreover, since each waveform is uniquely determined by a combination of the system parameters and initial conditions, each waveform can be stored with six system parameters.

II. Time Scaling Solutions of the Lorenz Equations

The Lorenz system, as given in Eq. 1, is one of the most well-studied chaotic systems [Strogatz, 1994; Cuomo, 1994; Guckenheimer & Holmes, 1983].

$$
\begin{aligned}
\dot{x} &= \sigma(y - x) \\
\dot{y} &= rx - y - xz \\
\dot{z} &= xy - bz
\end{aligned}
\tag{1}
$$

In order for the Lorenz system to give rise to chaotic dynamics, the Lorenz parameters σ, r, and b must satisfy Eqs. 2 - 4.

$$
b > 0
\tag{2}
$$

$$
\sigma > b + 1
\tag{3}
$$

$$
r > \frac{\sigma(\sigma + b + 3)}{(\sigma - b - 1)} \equiv r_c.
\tag{4}
$$

The variable r_c in the above equation is the critical value for r.

In this section, two techniques useful in generating time-scaled solutions to the Lorenz equations are presented. The first technique modifies the Lorenz equations so that the resulting solutions exactly equal time-scaled solutions of the original system. The second technique gives rise to approximately time-scaled solutions by scaling the Lorenz parameters.

To simplify the representation of the Lorenz equations, we use the vector $\underline{x}$, as defined in Eq. 5, to denote the x, y, and z state variables and use the vector f($\underline{x}$), as defined in Eq. 6, to denote the Lorenz equations.

$$
\underline{x} = \begin{pmatrix} x \\ y \\ z \end{pmatrix}.
\tag{5}
$$

$$f(\underline{x}) \;=\; \begin{pmatrix} \sigma(y - x) \\ rx - y - xz \\ xy - bz \end{pmatrix}. \tag{6}$$

With this notation, the Lorenz system in Eq. 1 is expressed as

$$\dot{\underline{x}} = f(\underline{x}). \tag{7}$$

A. Exactly Time-Scaling the Lorenz Equations

Using the above notation, a slightly modified Lorenz system is presented in Eq. 8 where $a > 0$. As can be seen in Eq. 8, the original Lorenz equations are scaled by a. The solutions, $\underline{x}_1(t)$, of Eq. 8 equal time-scaled solutions to the Lorenz equations, $\underline{x}(at)$, for identical initial conditions[1], i.e.

$$\dot{\underline{x}}_1 \;=\; af(\underline{x}_1) \tag{8}$$

$$\underline{x}_1(t) \;=\; \underline{x}(at). \tag{9}$$

The fact that the system in Eq. 8 gives rise to time-scaled solutions of the Lorenz equations, Eq. 9 can be verified by differentiating $\underline{x}_1(t)$ and using the chain rule to obtain

$$\dot{\underline{x}}_1(t) \;=\; \frac{d[\underline{x}(at)]}{d[at]} a$$

Substituting $f(at)$ for $\frac{d[\underline{x}(at)]}{d[at]}$ and using Eq. 9 results in

$$\dot{\underline{x}}_1 \;=\; af(\underline{x}_1(t)) \tag{10}$$

The time dependence can be dropped for notational convenience to yield the differential equations in Eq. 8, which shows that these equations are the differential equations yielding the solutions in Eq. 9.

The time-domain relationship in Eq. 9 also implies a frequency-domain relationship between the Fourier transform of $\underline{x}(t)$ and $\underline{x}_1(t)$. Specifically, a time scaling by a results in a frequency scaling by $\frac{1}{a}$. Correspondingly, the bandwidth of $\underline{x}_1(t)$ increases by a factor of a as the value of a in Eq. 8 increases. This bandwidth scaling is a useful property when generating radar waveforms.

B. Approximate Time-Scaling of the Lorenz Equations through the Lorenz Parameters

In this section, appropriate selection of the Lorenz parameters is shown to result in an approximate time and amplitude scaling of the Lorenz solutions. A system that corresponds exactly to a time and amplitude scaling is given in Eq. 11. As expressed in Eq. 12, solutions to Eq. 11, $\underline{x}_2(t)$, are equal to time and amplitude scaled solutions

---

[1]Even though this relationship is exact, due to rounding in the numerical integration methods and to the divergence of nearby Lorenz trajectories, numerically demonstrating the relationship in Eq. 9 is difficult if the magnitude of a is too large.

to the Lorenz equations if the initial conditions are related as in Eq. 13. These equations can be verified as was done previously with Eqs. 8-9.

$$\dot{\underline{x}}_2 = a^2 f(\frac{1}{a}\underline{x}_2) = \begin{pmatrix} a\sigma(y_2 - x_2) \\ arx_2 - ay_2 - x_2 z_2 \\ x_2 y_2 - ab_2 z_2 \end{pmatrix} \tag{11}$$

$$\underline{x}_2(t) = a\underline{x}(at) \tag{12}$$

$$\{x_2(0), y_2(0), z_2(0)\} = \{ax(0), ay(0), az(0)\} \tag{13}$$

Equating Eq. 11 to a Lorenz system of the form of Eq. 1 with parameters $\hat{\sigma}$, $\hat{r}$, $\hat{b}$ would require that

$$\begin{pmatrix} \hat{\sigma} \\ \hat{r} \\ \hat{b} \end{pmatrix} = \begin{pmatrix} a\sigma \\ ar - \frac{\hat{y}}{\hat{x}}(a-1) \\ ab \end{pmatrix}. \tag{14}$$

Consequently, a choice for a constant $\hat{r}$ does not exist, and the Lorenz parameters cannot be chosen to exactly time and amplitude scale the corresponding solutions.

However, when the term $\frac{\hat{y}}{\hat{x}}(a-1)$ in Eq. 14 is negligible for most values of t, then selecting $\hat{\sigma} = a\sigma$, $\hat{r} = ar$, and $\hat{b} = ab$ results in solutions $\hat{\underline{x}}(t)$ where $\hat{\underline{x}}(t) \approx \underline{x}_2(t) = a\underline{x}(at)$. In [Willsey, 2006], the term $\frac{\hat{y}}{\hat{x}}(a-1)$ is determined to be negligible when

$$\begin{aligned} r &\geq 360 \\ a &\in [0.4, \infty) \end{aligned} \tag{15}$$

Summarizing, we choose

$$\{\hat{\sigma}, \hat{r}, \hat{b}\} = \{a\sigma, ar, ab\} \tag{16a}$$

with

$$\{\hat{x}(0), \hat{y}(0), \hat{z}(0)\} = \{ax(0), ay(0), az(0)\} \tag{16b}$$

and the constraints in Eq. 15, in which case

$$\hat{\underline{x}}(t) \approx a\underline{x}(at) \tag{17}$$

To illustrate time-scaling through the use of a parameter scaling, two Lorenz systems with scaled parameters were numerically integrated (using a 4th order Runge-Kutta method with a step size of 10^{-3} seconds) and compared. The first system has a set of parameters $\{\sigma, r, b\}$ equal to $\{267, 595, 100\}$. A set of initial conditions were found on the attractor of this Lorenz system and were used to generate the x state variable which is shown with a solid line in Fig. 1. The parameters and the initial conditions of the second system were chosen according to Eq. 16 with $a = 0.95$. The x state variable of the second system is plotted with a dashed line in Fig. 1. As expected, the signal
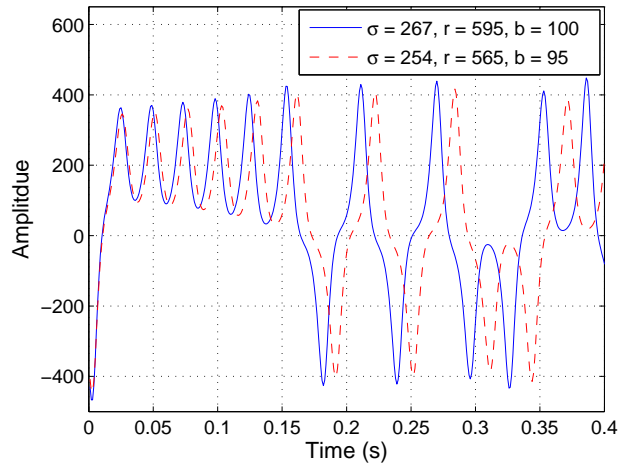
Fig. 1.   Time Evolution of the x State-Variable for Two Lorenz Systems. The two systems have different parameter sets that give rise to two Lorenz systems where one system is a time-scaled and re-normalized version of the other system. The time-scaling and re-normalization factor was 0.95.

represented with the dashed line is time and amplitude scaled by a factor of 0.95 when compared to the signal represented with the solid line[2]. Although only $x(t)$ is shown, $y(t)$ and $z(t)$ are similarly scaled[3].

III. SELECTING THE LORENZ SYSTEM PARAMETERS FOR WAVEFORM GENERATION

A typical radar waveform $s(t)$ is a real signal of the form shown in Eq. 18 (with $a(t)$ and $\theta(t)$ slowly varying relative to ω_c), and the spectral content of these signals is concentrated around $\pm\omega_c$ [Rihaczek, 1996].

$$s(t) = a(t)\cos(\omega_c t + \theta(t)) \tag{18}$$

The corresponding complex envelope, $\mu(t)$, and the transmit waveform, $s(t)$ are related as shown in Eq. 19[4].

$$s(t) = \Re\{\mu(t)e^{j\omega_c t}\} \tag{19}$$

All of the waveforms presented in this paper are used as the complex envelope.

The radar waveforms are extracted from the Lorenz system as a normalized, time-windowed segment of the x state variable[5]. The Lorenz waveform, $x_L(t)$, is expressed mathematically in Eqs. 20 and 21 where T denotes the

---

[2]Since the time and amplitude scaling is approximate, the two trajectories will eventually diverge as a result of a chaotic system's sensitivity to initial conditions.

[3]It is worth noting that although an exact time scaling via the Lorenz parameters is not attainable, the Lorenz system can be changed to give other chaotic systems with solutions that can be exactly time scaled by scaling its system parameters. Such systems are proposed in [Willsey, 2006].

[4]For a more detailed discussion of this analytic formulation of transmit waveform, see Chapter 2 of [Rihaczek, 1996].

[5]Based on preliminary studies, $x(t)$ was shown to lend itself best to waveform design when compared to the other state variables or combinations of state variables.

length of the waveform in time and x_p denotes the maximum of $|x(t)|$ over the time interval $t \in [0, T]$.

$$x_L(t) = \frac{1}{x_p} w_r(t) x(t) \tag{20}$$

$$w_r(t) = \begin{cases} 1; & t \in [0, T] \\ 0; & else \end{cases} \tag{21}$$

These waveform can also be generated with arbitrary time lengths and bandwidths. An additional benefit to these Lorenz waveforms is that, due to the uniqueness of solutions, each Lorenz waveform is uniquely specified by the initial conditions, the time length, and the Lorenz parameters, which allows for convenient compression and storage of the entire waveform that was generated in terms of a very small number of parameters. The remaining focus of this section is to select the Lorenz parameters so that the waveforms generated from the Lorenz system have the desired radar waveform properties.

A. Decoupling the Lorenz Parameters

As shown in Sec. II, scaling the system parameters approximately scales in time and amplitude the Lorenz solutions, and therefore also scales the bandwidth. For most parameter values, the Lorenz parameters can be decoupled such that one parameter primarily determines the bandwidth and the other two parameters control other radar waveform properties. This decoupling simplifies the determination of the desired waveform properties.

To decouple the Lorenz parameters so that one parameter controls bandwidth and the other two are used to control other waveform properties, we introduce the scaling parameters a, K and express σ, r, and b in Eq. 1 as

$$\sigma = a\sigma_0$$
$$r = ar_0 \tag{22}$$
$$b = aK$$

By first selecting K in $b = aK$, all combinations of $\{\sigma, r, b\}$ can be reached by varying σ_0, r_0, and a. When the constraints in Eq. 15 hold, varying a is interpreted as scaling the bandwidth by a, as discussed in Sec. II. As discussed below, the relevant combinations of system parameters for waveform generation satisfy Eq. 15.

In the next two sections, the Lorenz parameter space is explored. For this discussion the value of K is chosen to be 100, and the values of σ_0 and r_0 in Eq. 23 are varied to improve the average transmit power and range sidelobes of the radar waveform.

$$\{\sigma, r, b\} = a \cdot \{\sigma_0, r_0, 100\} \tag{23}$$

After determining σ_0 and r_0, a can be varied to give the desired system bandwidth.

B. Average Transmit Power

Many practical radar systems have peak power limitations. Consequently, transmit waveforms are usually designed with an average transmit power within a few dB of peak power. The peak-to-RMS ratio (PRMS) of the Lorenz
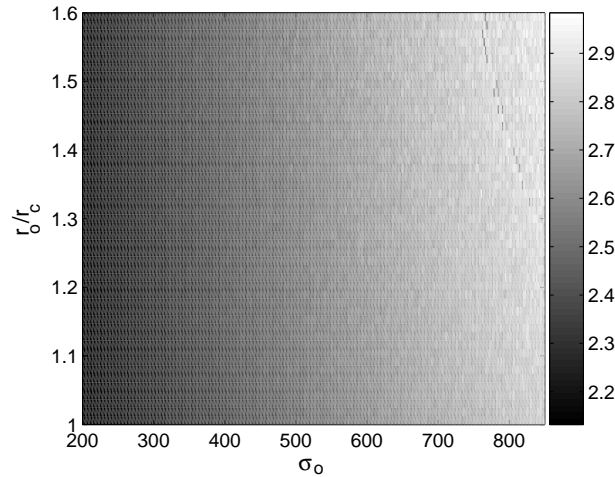
Fig. 2. Averaged Peak-to-RMS Ratio of Lorenz waveforms for Combinations of σ_0 and r_0. The variable r_c is the critical value for r.

waveforms, which are used as the complex envelope $\mu(t)$, quantifies this loss from peak transmit power. A low value for PRMS is desired.

The Lorenz parameters can be varied to reduce the PRMS ratio of Lorenz waveforms. With $a = 1$ in Eq. 23, the PRMS is explored for $\sigma_0 \in (200, 850)$ and $r_0 \in (r_c, 1.6r_c)^6$ (where r_c is given in Eq. 4). Using each combination of σ_0 and r_0, three distinct, 100 second Lorenz waveforms are generated with randomly selected initial conditions. The PRMS value associated with that combination of parameters is then determined by averaging the PRMS value over three trials. The results are shown in Fig. 2. As shown in Fig. 2, the PRMS is lowest in the lower, left-hand corner when both σ_0 and r_0 are reduced. In [Willsey, 2006], this PRMS variation is shown to be influenced by the underlying Lorenz dynamics also dependent on the Lorenz parameters.

C. Range Sidelobes

Since many practical radar systems utilize matched filters, the autocorrelation function, as defined in Eq. 24 is a critical design consideration[7]:

$$r_{\mu\mu}(t) \quad = \quad \int_{-\infty}^{\infty} \mu(\tau)\mu^*(\tau - t)d\tau. \tag{24}$$

Since the time scale of the matched-filter response is proportional to range separation between the target and the radar, autocorrelation function sidelobes correspond to sidelobes in range. Thus, low autocorrelation-function sidelobes prevent false alarms and also prevent larger targets from interfering with smaller targets. For Lorenz waveforms, the magnitude of the peak side-lobe of the autocorrelation function can be reduced by appropriately selecting the system parameters.

---

[6]Preliminary empirical studies indicated that these ranges were most relevant to waveform design.

[7]To simplify this discussion, the Doppler effect has been ignored.
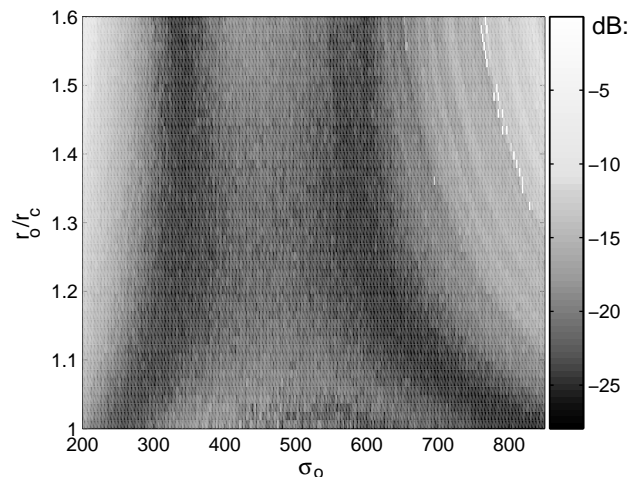
Fig. 3. Peak Side-lobe of the Lorenz System for Various Combinations of σ_0 and r_0 in Eq. 23 with $a = 1$.

The relationship between the peak side-lobe and the Lorenz parameters, as defined in Eq. 23, is determined empirically for various combinations of $\sigma_0 \in (200, 850)$ and $r_0 \in (r_c, 1.6r_c)$[8] while $a = 1$. For each combination of σ_0 and r_0, the peak autocorrelation function side-lobe is determined by averaging the peak side-lobe of three distinct Lorenz waveform with randomly selected initial conditions. The results are shown in Fig. 3, which illustrates that a region exists that corresponds to a minimum peak side-lobe.

The connection between the peak autocorrelation function side-lobe and the Lorenz parameters is further illustrated in Fig. 4. In this plot, the autocorrelation function corresponding to two different sets of system parameters are compared. The first set of system parameters, $\{\sigma = 262, r = r_c, b = 100\}$, lies in the darkest-shaded, low side-lobe region of Fig. 3; whereas, the second set of parameters, $\{\sigma = 262, r = 1.6 \cdot r_c, b = 100\}$, lies in a region corresponding to a relatively high peak side-lobe. As expected the peak side-lobe associated with the first set of system parameters is lower than the peak side-lobe associated with the second set of parameters. The dependence of the peak side-lobe on the Lorenz parameters results from underlying Lorenz system properties as discussed in [Willsey, 2006][9].

D. Design Curves for the Lorenz Parameters

By using Fig. 2 and Fig. 3, the values of σ_0 and r_0 in Eq. 23 can be chosen to trade off the peak-to-RMS ratio with the peak autocorrelation function side-lobe. This trade-off is illustrated with the design curves for $x_L(t)$

---

[8]Preliminary studies indicated that these ranges were most relevant to waveform design.

[9]In summary, as a trajectory moves around one wing of the Lorenz attractor, there is a probability, p, at which the trajectory transitions to the other wing of the attractor and a probability $(p - 1)$ at which the trajectory remains on the same wing of the attractor. The value of p is empirically shown to depend on the Lorenz parameters, and the Lorenz parameters corresponding to $p = 0.5$ are shown to also be the parameters that correspond to the minimum peak side-lobe.
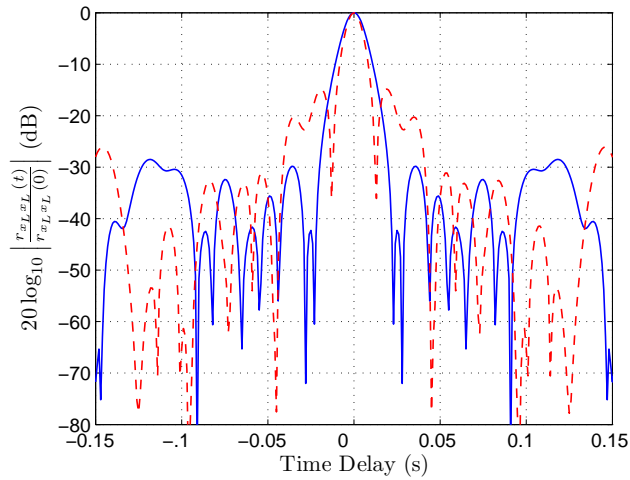
Fig. 4. Comparison of Two Normalized Autocorrelation Functions, $r_{x_L x_L}$, from Two Systems with Different System Parameters. The solid blue curve illustrates the autocorrelation function for the Lorenz parameters, $\{\sigma = 262, r = r_c, b = 100\}$, that correspond to a minimal peak autocorrelation function side-lobe. The dashed red curve illustrates the autocorrelation function for the Lorenz parameters, $\{\sigma = 262, r = 1.6 \cdot r_c, b = 100\}$, that correspond to a relatively high peak side-lobe.

shown in Fig. 5. The solid line, C_1, represents the combinations of σ_0 and r_0 that give rise to Lorenz waveforms with autocorrelation functions possessing minimized peak sidelobes. The three dashed lines represent combinations of σ_0 and r_0 that give rise to Lorenz waveforms with a peak-to-RMS ratio roughly equal to 2.2, 2.3, and 2.4, respectively. As depicted in Fig. 2, the peak-to-RMS ratio of the Lorenz waveform monotonically increases from the bottom left corner of Fig. 5 to the top right corner. When generating $x_L(t)$, combinations of σ_0 and r_0 will be chosen on C_1 below the line corresponding to a peak-to-RMS less than 2.3. These combinations of parameters are illustrated in the figure as the operating region, which is the shaded portion of C_1[10]. Finally, the parameter a in Eq. 23 can be varied to set the bandwidth of the resulting Lorenz waveform.

IV. DISCUSSION ON THE RESULTING LORENZ WAVEFORMS

The Lorenz waveforms described in this paper possess many properties that make them well-suited for several applications. With large bandwidths and long time lengths, waveforms from the Lorenz system possess sharp autocorrelation functions capable of achieving high range resolution and low range sidelobes. Furthermore, waveform generation with the Lorenz system is useful in generating a large set of nearly orthogonal waveforms (as described in [Willsey et al., 2010]) for applications such as those relevant to MIMO radar systems [Robey et al., 2004]. As described in Sec. III, these waveforms can be generated with arbitrary time lengths and bandwidths, and each of these waveforms can be represented with only a few, finite-precision system parameters. Finally, since scaling the

[10]All lines in Fig. 5 are drawn with a relatively large width to indicate that the combinations of σ_0 and r_0 that give rise to minimized sidelobes and particular realizations of the peak-to-RMS ratio were numerically approximated (as opposed to analytically determined).
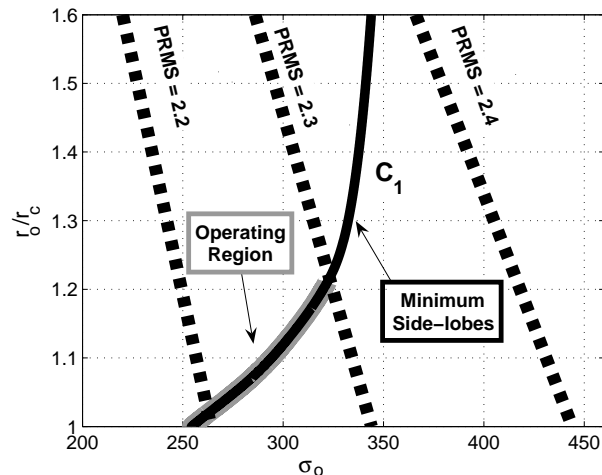
Fig. 5.   Lorenz Waveform Design Curves. For $b_0 = 100$, these curves indicate combinations of σ_0 and r_0 that tradeoff the peak-to-RMS ratio and magnitude of the peak side-lobe.

Lorenz parameters is shown to approximately time scale the Lorenz solutions, the potential exists for obtaining range and Doppler characteristics of a target by using scaled Lorenz parameters either with the self-synchronizing property in [Pecora & Carroll, 1991] or with a method similar to that presented in [Liu et al., 2007] with Chua's circuit.

Although the Lorenz parameters have been determined to achieve desirable radar waveform properties, an evaluation of these waveforms in [Willsey et al., 2010] suggests that they can be improved even further with the procedure in [Willsey et al., 2010]. This improvement results in radar waveforms based on the Lorenz system that possess low range sidelobes, an average power within a few dB of peak power, and limited spectral leakage. Plots of the corresponding autocorrelation function and energy spectrum are depicted in [Willsey et al., 2010]. Figure 6 from [Willsey, 2006] depicts a typical transmit signal to illustrate how the average power of the waveform is within a few dB of peak power.

V. CONCLUSIONS

In this paper, the relationship between the Lorenz parameters and the radar waveform properties of the Lorenz waveforms is explored. Selection of the Lorenz parameters is shown to vary the Lorenz waveform bandwidth - via a time and amplitude scaling - and is shown to trade-off the PRMS ratio with peak autocorrelation function side-lobe. Due to the naturally tapered spectrum and bounded dynamics of the Lorenz solutions, the resulting waveforms can be readily improved with the procedure in [Willsey et al., 2010].
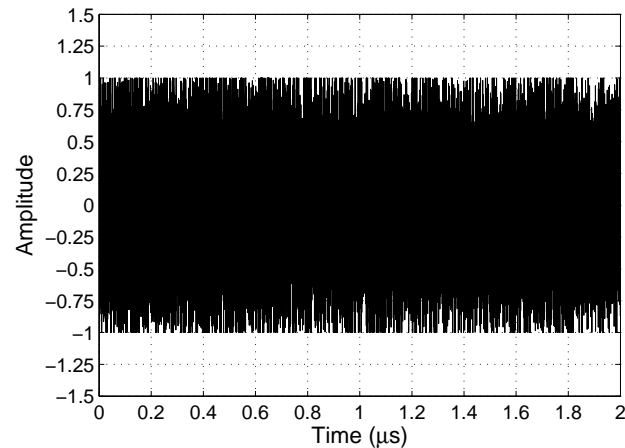
ACKNOWLEDGMENT

Fig. 6.   A Time Segment of a Radar Waveform Based on the Lorenz System. This waveform was originally generated as a Lorenz waveform and was improved with an improvement procedure in [Willsey et al., 2010] and [Willsey, 2006].

REFERENCES

North, D. O. [1963] "An analysis of the factors which determine signal-noise discrimination in pulsed carrier systems," RCA Lab., Rep. PTR-6C, reprinted in *Proc. IEEE*, **51**, 1016-1027.

Rihaczek, A. W. [1996] *Principles of High-Resolution Radar*, *Applied Mathematical Sciences*, **42**, Artech House, Norwood, Massachusetts.

Venkatasubramanian, V. & Leung, H. [2005] "A Novel Chaos-Based High-Resolution Imaging Technique and Its Application to Through-the-Wall Imaging," *IEEE Signal Processing Letters*, **12**, 528-531.

Lukin, K. A. [2001] "Millimeter wave noise radar applications: Theory and experiement," *Proc. MSMW*, 68-73.

Flores, B. C., Scolis, E. A. & Thomas, G. [2003] "Assessment of chaos-based FM signals for range-Doppler imaging," *IEE Proc. Radar Sonar Navig.*, **150**, 313-322.

Lorenz, E. N. [1963] "Deterministic nonperiodic flow." *Journal of the Atmospheric Sciences*, **20**, 130-141.

Willsey, M. S., Cuomo, K. M. & Oppenheim, A. V. [2010] "Quasi-Orthogonal Wideband Radar Waveforms Based on Chaotic Systems," to be published.

Strogatz, S. H. [1994] *Nonlinear Dynamics and Chaos*, Addison-Wesley.

Cuomo, K. M. [1994] "Analysis and syntesis of self-synchronizing chaotic systems," Doctoral thesis, Massachusetts Institute of Technology, 77 Massachusetts Avenue, Cambridge, MA 02139.

Guckenheimer, J. & Holmes, P. [1983] *Nonlinear Oscillations, Dynamical Systems, and Bifurcations of Vector Fields*, *Applied Mathematical Science*, **42**, Spinger-Verlag, New York, New York.

Willsey, M. S. [2006] "Quasi-Orthogonal Wideband Radar Waveforms Based on Chaotic Systems," Master of Engineering thesis, Massachusetts Institute of Technology, 77 Massachusetts Avenue, Cambridge, MA 02139.
    Available at: http://www.rle.mit.edu/dspg/documents/mattnewthesis.pdf

Robey, F. C., Coutts, S., Weikle, D., McHarg, J. C. & Cuomo, K. M. [2004], "MIMO radar theory and experimental results," in Signals, Systems and Computers, 2004, Conference Record of the Thirty-Eighth Asilomar Conference, Pacific Grove, CA.

Pecora, L. M. & Carroll, T. L. [1991] "Synchronization in chaotic systems," *Physical Review Letters*, **64**, 821-824.

Liu, Z., Zhu, X., Hu, W. & Jiang, F. [2007] "Principles of Chaotic Signal Radar," *International Journal of Bifurcation and Chaos*, **17**, 1735-1739.

Matt S. Willsey Matt S. Willsey attended the Massachusetts Institute of Technology where he received his B.S. degree in electrical science and engineering in 2005 and his M.Eng. degree in electrical engineering and computer science in 2007.

Mr. Willsey was a graduate student at the Research Laboratory of Electronics at M.I.T. during this project, and his research interests included waveform design, nonlinear dynamics, and MIMO radar systems. He is currently employed as an Engineering Scientist at the Applied Research Laboratories, the University of Texas at Austin (ARL:UT). At ARL:UT, his his research is focused on signal processing applications for sonar systems. He was the recipient of the Siebel Scholarship in 2005 and is a member of Tau Beta Pi, Eta Kappa Nu, and Sigma Xi.

Kevin M. Cuomo Kevin M. Cuomo received the B.S. (magna cum laude) and M.S. degrees in electrical engineering from the State University of New York (SUNY) at Buffalo, in 1984 and 1986, respectively, and the Ph.D. degree in electrical engineering from Massachusetts Institute of Technology (MIT), Cambridge, in 1994.

He is a Senior Staff Member in the Ranges and Test Bed Group, MIT Lincoln Laboratory, where he works on the development of advanced signal processing methods for various radar applications. Before joining Lincoln Laboratory in 1988, he was a member of the research staff at Calspan Corporation, Buffalo, NY. He has authored several technical papers and reports in the areas of super resolution data processing and applications of chaotic dynamical systems for radar and communications. Recent research efforts include the development of super orthogonal waveforms for Multiple-Input Multiple-Output (MIMO) radar and corresponding beam space signal processing techniques.

Dr. Cuomo was awarded Departmental Honors and was the recipient of a University Fellowship and a Hughes Fellowship while attending SUNY Buffalo. He is a member of Tau Beta Pi, Eta Kappa Nu, and Sigma Xi.

Alan V. Oppenheim Alan V. Oppenheim was born in New York, New York on November 11, 1937. He received S.B. and S.M. degrees in 1961 and an Sc.D. degree in 1964, all in Electrical Engineering, from the Massachusetts Institute of Technology. He is also the recipient of an honorary doctorate from Tel Aviv University.

In 1964, Dr. Oppenheim joined the faculty at MIT, where he is currently Ford Professor of Engineering. Since 1967 he has been affiliated with MIT Lincoln Laboratory and since 1977 with the Woods Hole Oceanographic Institution. His research interests are in the general area of signal processing and its applications. He is coauthor of the widely used textbooks Discrete-Time Signal Processing and Signals and Systems. He is also editor of several advanced books on signal processing.

Dr. Oppenheim is a member of the National Academy of Engineering, a fellow of the IEEE, and a member of Sigma Xi and Eta Kappa Nu. He has been a Guggenheim Fellow and a Sackler Fellow. He has received a number of awards for outstanding research and teaching, including the IEEE Education Medal, the IEEE Jack S. Kilby Signal Processing Medal, the IEEE Centennial Award and the IEEE Third Millennium Medal. From the IEEE Signal Processing Society he has been honored with the Education Award, the Society Award, the Technical Achievement Award and the Senior Award. He has also received a number of awards at MIT for excellence in teaching, including the Bose Award and the Everett Moore Baker Award.